Traveling waves in an optimal velocity model of freeway traffic

Peter Berg[1,*] and Andrew Woods[2,†]
[1]*School of Mathematics, University of Bristol, University Walk, Bristol BS8 1TW, United Kingdom*
[2]*BP Institute, Bullard Laboratories, University of Cambridge, Madingley Road, Cambridge CB3 0EZ, United Kingdom*
(Received 24 August 2000; published 21 February 2001)

Car-following models provide both a tool to describe traffic flow and algorithms for autonomous cruise control systems. Recently developed optimal velocity models contain a relaxation term that assigns a desirable speed to each headway and a response time over which drivers adjust to optimal velocity conditions. These models predict traffic breakdown phenomena analogous to real traffic instabilities. In order to deepen our understanding of these models, in this paper, we examine the transition from a linear stable stream of cars of one headway into a linear stable stream of a second headway. Numerical results of the governing equations identify a range of transition phenomena, including monotonic and oscillating travelling waves and a time-dependent dispersive adjustment wave. However, for certain conditions, we find that the adjustment takes the form of a nonlinear traveling wave from the upstream headway to a third, intermediate headway, followed by either another traveling wave or a dispersive wave further downstream matching the downstream headway. This intermediate value of the headway is selected such that the nonlinear traveling wave is the fastest stable traveling wave which is observed to develop in the numerical calculations. The development of these nonlinear waves, connecting linear stable flows of two different headways, is somewhat reminiscent of stop-start waves in congested flow on freeways. The different types of adjustments are classified in a phase diagram depending on the upstream and downstream headway and the response time of the model. The results have profound consequences for autonomous cruise control systems. For an autocade of both identical and different vehicles, the control system itself may trigger formations of nonlinear, steep wave transitions. Further information is available [Y. Sugiyama, *Traffic and Granular Flow* (World Scientific, Singapore, 1995), p. 137].

DOI: 10.1103/PhysRevE.63.036107 PACS number(s): 45.70.Vn, 89.40.+k, 02.60.Cb

I. INTRODUCTION

Increasing congestion and travel times are forcing a further extension of the road network. Nowadays, due to environmental pressure, a compromise lies in the application of technologies to optimize the efficiency of existing roads with respect to throughput and speed. Monitoring freeways and on-line traffic data provide important information for these projects which are based on mathematical models of traffic flow [1].

Hitherto the aim of these models was to reproduce phenomena of traffic such as flow breakdown, stop-and-go traffic and the speed of shock waves traveling upstream and causing rapid breaking. One approach is a car-following model. It consists of a dynamic equation for the speed of every car depending on its current speed, its inertia, the driver's reaction time, the headway to the car in front and the changing of the latter with time. Since every single car is modeled, it belongs to the class of microscopic models.

The advantage of car-following models is that they both model traffic flow and have practical applications in form of autonomous cruise control systems (ACCS). These systems link each car to the preceding car via a follow-the-leader algorithm similar to the governing equation of a car-following model. The target is to enable high flux driving in stable and safe convoys. Insight into the phenomena associated with car-following models gives insight into ACCS. One common and fundamental process is the merging of a platoon of moving cars at one headway into a platoon moving with a second headway. This situation appears at bottlenecks and lane merging. It is important to know what transitions can possibly occur in the system to prevent instabilities and dangerous traffic situations.

In this paper we classify the rich variety of those transitions between different headways. We examine flows in the linearly stable regime of the Bando model [2], in which the acceleration of a car n is given by

$$\ddot{x}_n = \dot{v}_n = a[V(b_n) - v_n], \tag{1}$$

where x_n is the position of the car n, v_n its speed, and b_n its headway. The optimal velocity (OV) function

$$V(b) = \tanh(b-2) + \tanh(2) \tag{2}$$

describes the desired speed of a driver at a distance b behind the car in front. It is a monotonic increasing function with a maximum speed $V(b \to \infty)$ and $V(0) = 0$. This corresponds to ideal vehicles of length 0. The constant of proportionality, a, is called the sensitivity.

Bando *et al.* showed that the model is unstable in a headway range

$$b_{c_1} < b < b_{c_2} \tag{3}$$

for which

*Electronic address: Peter.Berg@bris.ac.uk (http://www.maths.bris.ac.uk).
†Electronic address: Andy@bpi.cam.ac.uk (http://www.bpi.cam.ac.uk).

 ©2001 The American Physical Society

$$\frac{2V'(b)}{a} > 1. \tag{4}$$

For these conditions an initial uniform flow breaks down under the slightest perturbation and turns into stop-and-go traffic. This is characterized by stable regions of high speed merging into regions of low speed so as to conserve total flux. The high and low speed flows are both in the stable regime. The shape of the traveling fronts of these clusters, their speed, the density inside and outside the cluster, as well as their outflow are characteristic parameters of traffic flow [3].

However, the dynamics of transitions in the two stable regimes

$$b < b_{c_1} \tag{5}$$

and

$$b > b_{c_2} \tag{6}$$

have received less attention. Here, we examine the richness of behavior which may develop when one stream merges into a second. This is a generalization of the nonlinear transition waves found in these earlier studies and provides new insight into the selection of nonlinear stop-go waves. In Sec. II we identify different transition phenomena as the size of headway jump across the transition varies. Section III relates a nonlinear wave type of the stable regime to the stop-and-go jam fronts of unstable flow. Although the main part of our study uses the Bando car-following model, we include some calculations in Sec. IV using another OV function suggested by Herrmann and Kerner [4] which reproduces all the qualitative features of data from the German autobahn although some quantitative details are different. This is to see whether the range of wave types found in Sec. II are an intrinsic feature of car-following models based on a relaxation term. In Sec. V we make some remarks on the possible impact of this transition classification on bottlenecks and ACCS. A brief discussion of a more realistic convoy of multi-species vehicles follows in the Appendix.

II. TRAVELING WAVES OF THE STABLE REGIME

The transition between traffic flows of different throughput is a well observed phenomenon. Bottlenecks, speed limits, cars entering a jam or emerging from it are typical situations. Here, we study transitions which occur in freely moving traffic without local speed limits or any other artificial hindrance due to road layout. We expect the transitions that evolve to travel along the road either up or down stream. Their direction and shape depend on the OV function and the sensitivity.

If the governing Eq. (1) is divided by a, it reads

$$\frac{1}{a}\dot{v}_n = V(b_n) - v_n. \tag{7}$$

This shows that the inverse of the sensitivity can be interpreted as the inertia of cars. From the instability criterion Eq. (4) it is clear that a platoon of cars is more stable the smaller the inertia is. Heavier vehicles of higher inertia, which cannot react sufficiently fast to changing traffic situations, are more likely to cause flow breakdown. We therefore study traveling waves with increasing sensitivity a corresponding to more stable flow. At $a=2.0$ the flow is just on the verge of instability.

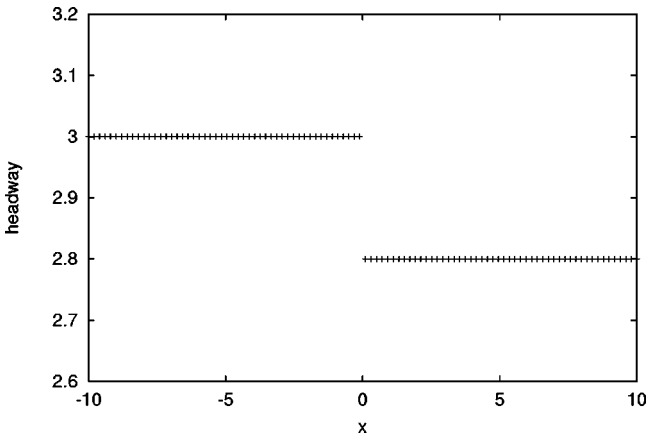

FIG. 1. Initial conditions ($t=0$): various wave types evolve from a discrete jump in headway (Fig. 1).

In our analysis we consider transitions which evolve from initial conditions similar to Fig. 1. The jump of headway is determined by the boundary conditions $b_- = b(x \to -\infty)$ and $b_+ = b(x \to \infty)$. We prefer to present the figures with lines rather than with dots representing each car. This simplifies comparisons of traveling wave solutions (Fig. 2).

A. Transition involving a decrease in headway: Decelerating traffic

Once the optimal velocity function V is given, the only remaining parameter in the system is the sensitivity a. For different a the analysis of the wave fronts in terms of upstream and downstream headways can be summarized in a diagram as shown in Fig. 2. On the verge of instability ($a=2.0$), decelerating traffic can be classified in six categories. There are monotonic (region I), oscillatory (region II), and dispersive transitions (region III). These can be explained by looking at the fundamental diagram of this model (Fig. 3) which describes stationary, homogeneous flow situations [$\dot{v}_n \equiv 0 \Rightarrow v_n = V(b_n) = V(b)$]. The solid line illustrates the flow q as a function of the density $\rho = 1/b$,

$$q(\rho) = \rho v(\rho) \Rightarrow q(1/b) = \frac{V(b)}{b}. \tag{8}$$

In case of a monotonic traveling wave solution (shock wave of region I), both up and down stream headways are greater than the turning point $b_{\mathrm{tp}} = 2.0$ and occur at a density ρ that is smaller than the turning point $\rho_{\mathrm{tp}} = 1/b_{\mathrm{tp}} = 0.5$ (Fig. 3). We can interpret this result in the limit $a \gg 1$. Then the Bando model corresponds to the continuum model of Lighthill and Whitham [5]

$$\rho_t + q_x = \rho_t + (\rho V(1/\rho))_x = 0. \tag{9}$$

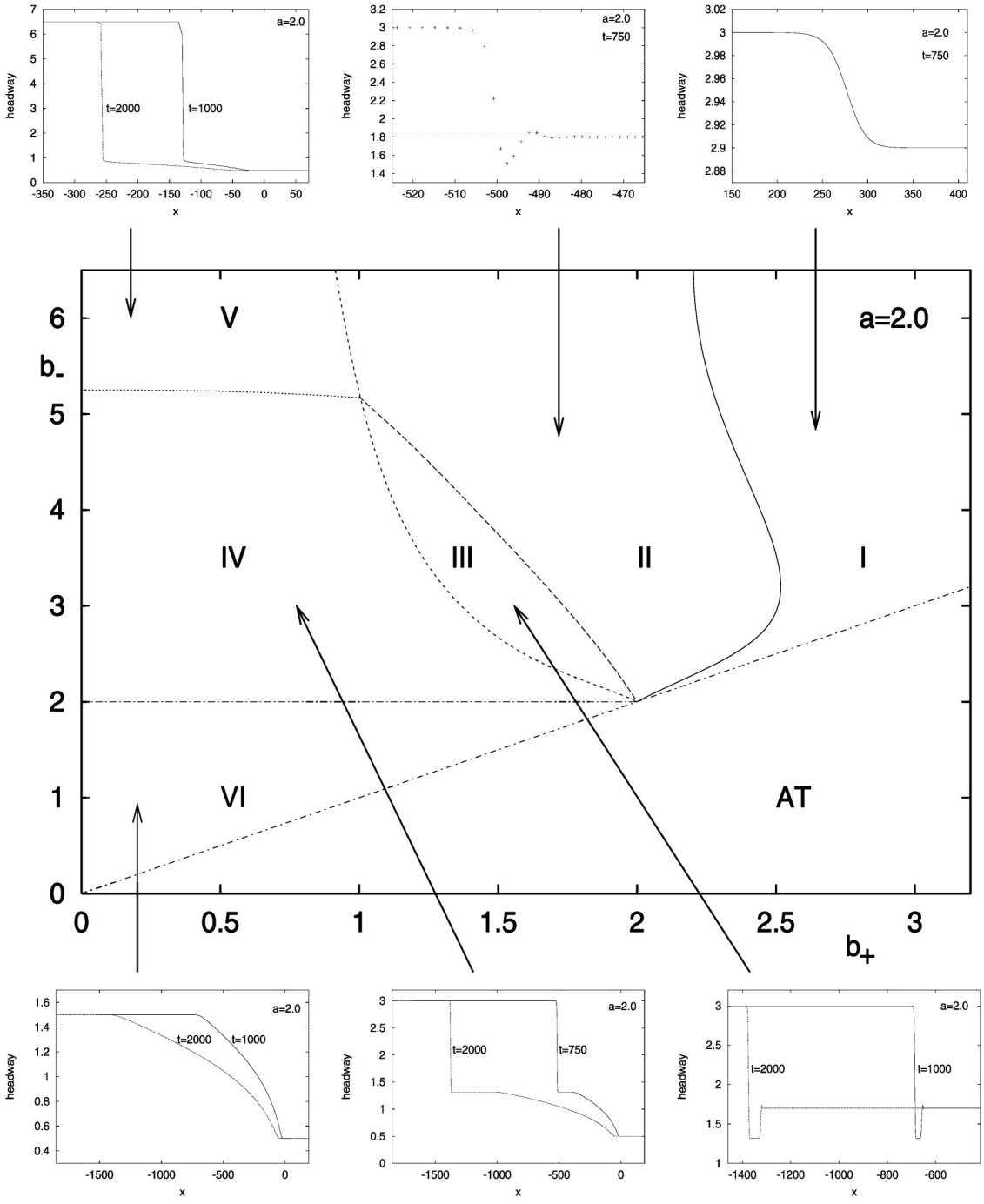

FIG. 2. Transitions of decelerating traffic ($a=2.0$) derived from numerical data: I: monotonic, II: oscillatory, III: Bando wave and second shock wave, IV: Bando wave, plateau and dispersive tail, V: jump and dispersive tail for large jumps in headway, VI: purely dispersive; AT: region of accelerating traffic (Fig. 5).

For this model the method of characteristics shows that the local wave speed $c(\rho)$ is given by the slope of the tangent of the fundamental diagram at its corresponding density

$$c(\rho)=q_{\rho}(\rho). \tag{10}$$

For densities greater than the density $\rho_{\mathrm{mf}}=1/3$ of maximum flow the slopes are negative and the information travels upstream.

For waves of region I the local upstream wave speed as a function of position in the wave increases down the road. This leads to a shock wave solution where the wave speed is given by its upstream and downstream densities

$$c=\frac{q(\rho_{+})-q(\rho_{-})}{\rho_{+}-\rho_{-}}. \tag{11}$$

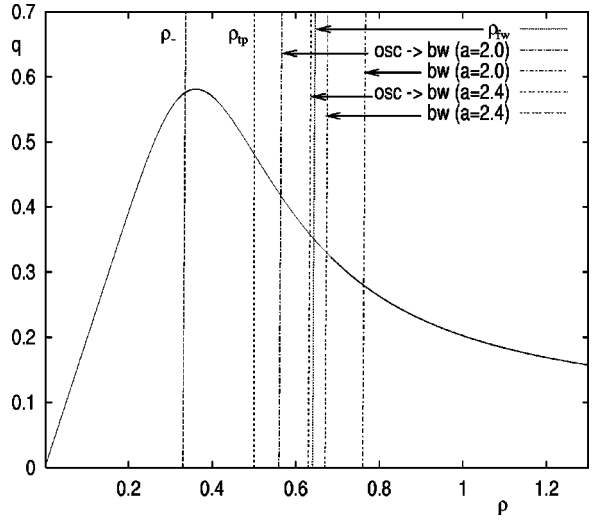

FIG. 3. Fundamental diagram: the transitions oscillatory wave → Bando wave (osc → bw) and the Bando wave (bw) itself approach the fastest wave with increasing a.

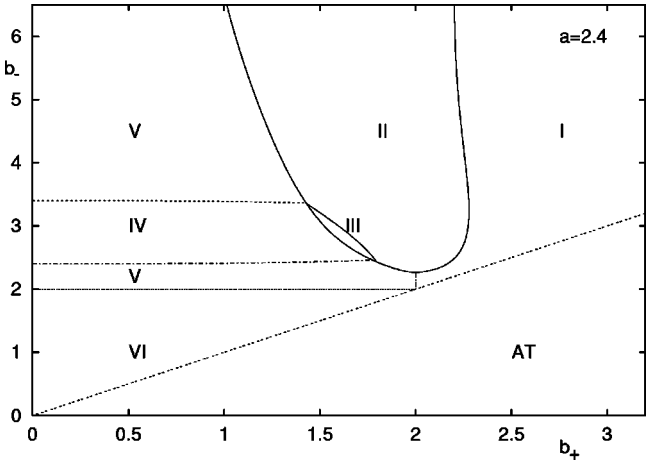

FIG. 4. Transitions of decelerating traffic ($a=2.4$): with increasing sensitivity regions III and IV shrink until they vanish. Region V spreads out between regions IV and VI. The region II of oscillatory waves shrinks too, since the traffic flow reacts faster to changes in headway due to lower inertia $\sim 1/a$.

For purely dispersive waves (region VI), both upstream and downstream densities are bigger than the turning point and the magnitude of the wave speed across the profile now decreases. This means that the speed of propagation of information decreases as one moves downstream. Hence drivers entering the transition react faster to the traffic situation than drivers further downstream. Therefore, the number of drivers who are part of the decelerating maneuver grows and a dispersive tail forms. A traveling wave solution does not exist in this regime.

The oscillatory waves (region II) always have an upstream density smaller than the turning point, but their downstream density can be smaller or bigger than the turning point. It is therefore not as straightforward to interpret the results. One has to be aware that the fundamental diagram shows the flow as a function of the density only for a steady flow. Generally, for nonstationary situations, the flow is not a function of the density any more. A given ρ might correspond to various flows depending on the traffic situation. Hence the wave speed is not a function of the density. One example is a traveling wave solution (region I). Every point along the profile has the same wave speed even though the density varies.

However, in the limit of transitions involving small changes of headway and with $a \to \infty$, we expect a monotonic transition, since cars assume their desired speed immediately and react sufficiently fast to the surrounding traffic situation. For greater jumps in headway and smaller values of the sensitivity, deviations from the monotonic adjustment occur as oscillatory waves in a similar fashion to the transition from overdamping to underdamping of a spring. With these larger changes in headway, the inertia of cars is too big to allow for simple monotonic transitions in flow.

However, when the jump in headway increases to a certain value the oscillations become so big that the wave jumps on to another solution (region III). It consists of two shock waves of different speeds with a growing region of slow moving traffic in between. This solution first jumps from the upstream headway b_- to an intermediate headway b_{bw}, represented by the dotted line between regions III and IV in Fig. 2, before it eventually matches the downstream headway through another shock wave. b_{bw} is a function of b_- and the sensitivity a and can only be determined numerically [6]. We refer to this nonlinear wave between the upstream headway b_- and the intermediate headway b_{bw} as a Bando wave. For all points of region III the solution consists of two shock waves of different speeds.

For lower downstream headways than b_{bw}, the transition involves a Bando wave followed by a plateau of increasing length with a dispersive tail (region IV). Transforming the headways of this graph, $b_-=3$ and $b_+=0.5$, into the fundamental diagram Fig. 3, the corresponding densities are rather far apart from each other with the turning point in between. Therefore, the magnitude of the local wave speed across a monotonic profile between these two headways firstly increases, leading to a shock wave, and then decreases, leading to a dispersive wave.

The wave profile we obtain consists of these two types of waves as expected, with a plateau $b_{\mathrm{pl}} \approx 1.3$ overshooting the turning point $b_{\mathrm{tp}}=2$ due to the inertia of cars. The plateau forms because the upstream speed of the shock wave is higher than the local speed of the dispersive tail at its onset. In terms of fluxes, the shock wave provides more cars per unit time (outflow of the shock wave) than cars beginning to break at the onset of the dispersive tail (inflow of the dispersive tail).

If the upstream headway is too big (region V), the difference of speed between the shock wave and the onset of the dispersive tail is negligible. The wave profile assumes a solution where the dispersive tail and the shock wave have the same speed and no plateau forms.

For higher sensitivities, equivalent to smaller inertia (Fig. 4), the cars react faster to the traffic situation. Therefore, the region of oscillatory waves, and hence Bando waves, shrinks until the latter eventually disappears. Monotonic and purely

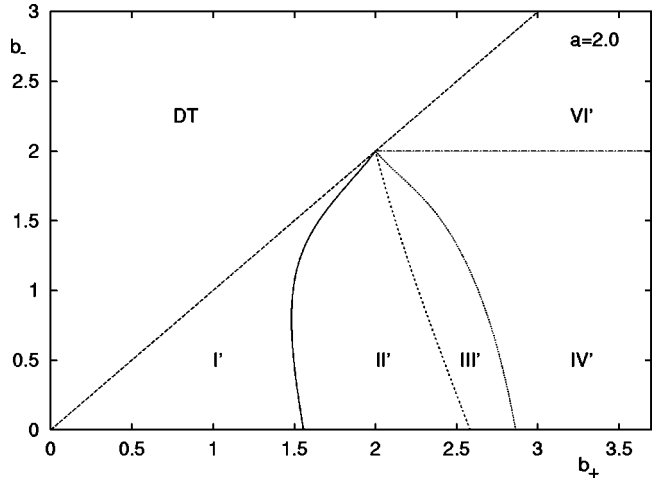

FIG. 5. Transitions of accelerating traffic ($a=2.0$): I′: monotonic, II′: oscillatory, III′: Bando wave and second shock wave, IV′: Bando wave, plateau and dispersive tail, VI′: purely dispersive; DT: decelerating traffic (Fig. 2); the wave phenomena are equivalent to decelerating traffic apart from a missing region V′ analogous to region V in Figs. 2 and 4.

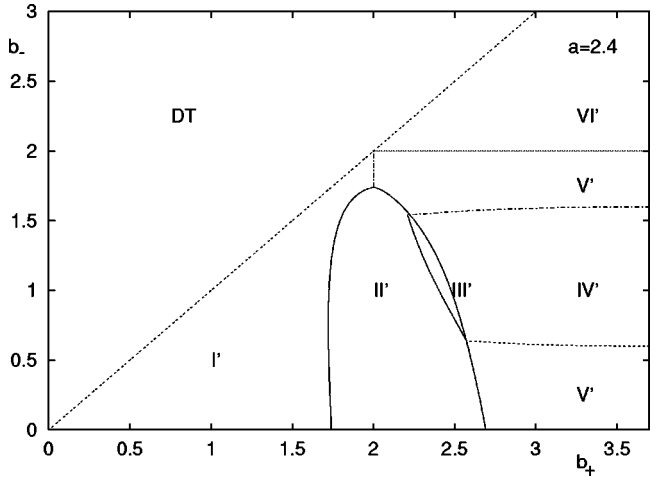

FIG. 6. Transitions for accelerating traffic ($a=2.4$): again, with increasing sensitivity regions III′ and IV′ shrink until they vanish. Similarly region V′ spreads out between regions IV′ and VI′ and eventually takes the place of region IV′.

dispersive waves (I and VI) still exist and waves of type V take the place of plateau waves (type IV). For large a, $a \gg 2.0$, four different wave types remain: monotonic (I), oscillatory (II), purely dispersive (VI), and shock wave plus adjoining dispersive tail without plateau in between (V).

B. Transition involving an increase in headway: Accelerating traffic

Once the diagrams for the wave types of decelerating traffic (Figs. 2 and 4) are worked out, those of accelerating traffic can be obtained by a mathematical transformation. By subtracting the governing equations (1) for two adjacent cars $n+1$ and n, we obtain the equation for the nth headway

$$\ddot{b}_n = a[V(b_{n+1}) - V(b_n) - \dot{b}_n]. \tag{12}$$

For the OV function, Eq. (2), this equation is invariant under the transformation

$$b' = 4 - b. \tag{13}$$

As a consequence the wave profiles are symmetric about $b=2$ and this relates accelerating and decelerating traffic. The diagrams showing the variety of the wave types associated with accelerating traffic (Figs. 5 and 6) are simply derived by reflecting the diagrams Figs. 2 and 4 at the point (2.0/2.0). Here, the dispersive region V' only appears for higher values of a (Fig. 6), because its upstream headway would be negative and hence meaningless (Fig. 5). Similarly we discover the same types of transitions and the disappearance of Bando waves and plateaus for sufficiently high a.

C. Fastest wave and Bando wave

For any given upstream headway b_- the model predicts a fastest traveling wave; this can be identified from the fundamental diagram.

For a headway b_-, equivalent to a density $\rho_- = 1/b_-$, the downstream density of the fastest wave is given by the extremum of the wave speed Eq. (11). Setting the first derivative to zero $[c'(\rho_+)=0]$ and excluding $\rho_- = \rho_+$ leads to

$$q'(\rho_+) = \frac{q(\rho_+) - q(\rho_-)}{\rho_+ - \rho_-} \tag{14}$$

which can be solved numerically for any OV function V. Equation (14) defines the maximum speed as the point where the chord $\rho_- \to \rho_+$ and the tangent at ρ_+ are identical. It does not necessarily mean that this traveling wave exists since the transition can also occur as a dispersive wave.

In Fig. 3 we choose $b_- = 3.0$ and find the fastest wave possible as the tangent of this point onto the flow curve. The downstream headway, $b_+ = 1.54$, of the fastest wave corresponds to a density $\rho_+ = 0.65$. As a increases the headway jump at which the oscillatory traveling wave (region II) is replaced by the Bando wave (region III) approaches the headway jump associated with the fastest wave. Similarly the headway jump at which the Bando wave (region III) is replaced by region IV also approaches the headway jump associated with the fastest wave. This is consistent with the shrinkage of region III (Figs. 2 and 4).

The curve of maximum speed Eq. (14) can now be added to Figs. 2 and 4 which yields Fig. 7. It shows that there are only two points where the fastest wave exists and these are the vertices of region III. For values of a greater than the bifurcation point, $a=2.43$, region III disappears and there are no Bando waves in the system. The fastest waves predicted by the fundamental diagram lie entirely in the dispersive regions V and VI. For values $2.0 \leqslant a \leqslant 2.43$, they are either part of the dispersive regimes V and VI or of the Bando wave regime III. In the latter case the solution jumps on to the slower Bando wave. We conclude that in the stable regime, $a \geqslant 2.0$, the fastest wave predicted by the fundamental diagram can only be found for two cases which correspond to the vertices of region III, the Bando wave region.

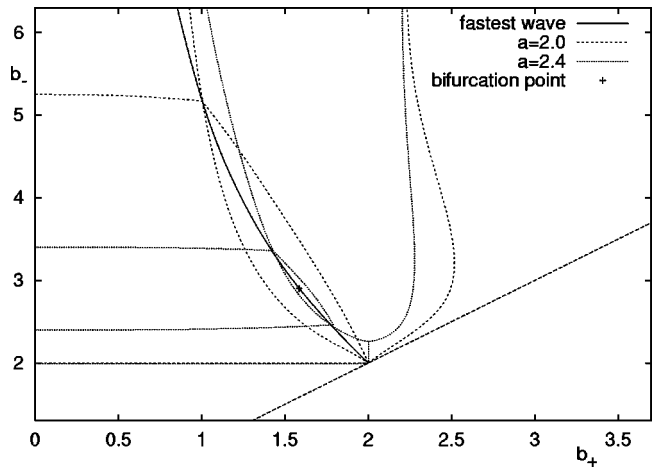

FIG. 7. For a given upstream headway b_- the fastest wave theoretically possible is either not accessible or just for two cases, Bando waves. Otherwise it is either part of region III (Bando wave) or of the dispersive domains V and VI.

Since this region disappears for large a, no fastest wave can be found for highly stable traffic, $a>2.43$.

III. STABLE AND UNSTABLE FLOW PATTERNS

In this section we show that the jam fronts of stop-and-go traffic correspond to two specific Bando wave solutions in the unstable regime.

Holland [7] investigated the plateau effect for unstable flow $a<2.0$. This can be discovered by setting up special road conditions as illustrated in Figs. 8 and 9. The first figure exhibits how an initial steady flow of uniform headway ($b_n \equiv 2.0$ at $t=0$) evolves, if the leading car approaches red traffic lights (X) and decelerates until it comes to a standstill at $x=0$. The wave profile of Fig. 9 evolves from the same initial conditions. Now the leading car accelerates at $t=0$ and $x=0$ from $v_{n=1}(t=0)=V(b=2)$ to maximum speed

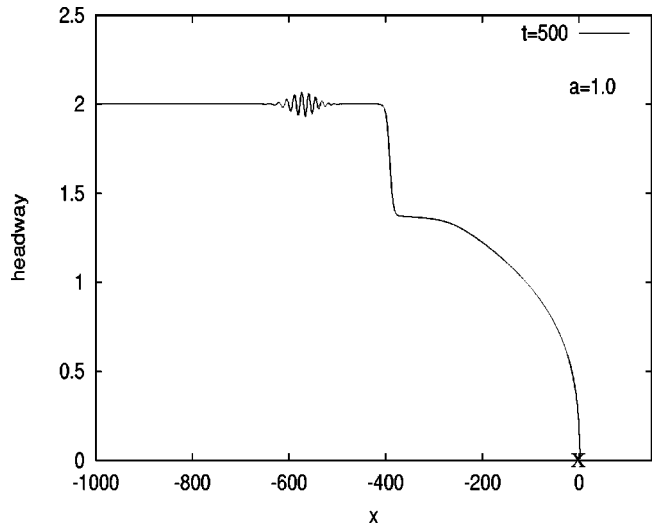

FIG. 8. Onset of instability: wave profile of a platoon of cars after $t=500$ and $a=1.0$ for an initial ($t=0$) homogeneous flow of headway $b=0$ and a leading car at $x=0$.

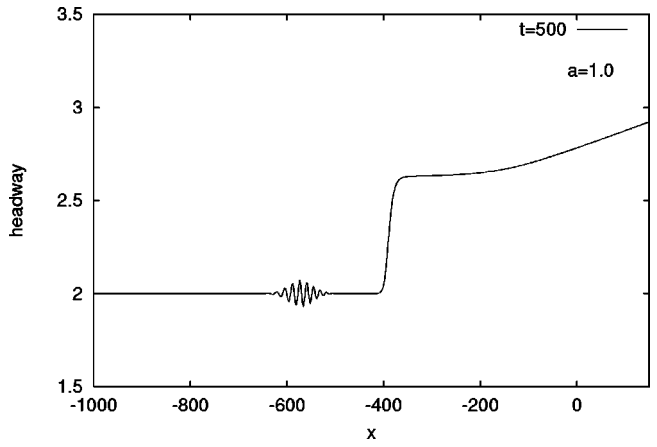

FIG. 9. Onset of instability: wave profile of a platoon of cars after $t=500$ and $a=1.0$ for a freely accelerating, leading vehicle at $x=0$ and $t=0$ from $b_-=2.0$.

$v_{n=1}(t\to\infty)=V(b\to\infty)=\tanh(\infty)+\tanh(2)$. This simulates the end of a temporal speed limit along a motorway. At $a=1.0$ the model is unstable for $b=2.0$ and after $t=500$ the oscillations in the platoon mark the onset of traffic breakdown. However, we can already observe the plateau effect.

Now one can set up a map, $b_{\rm pl}(b_-)$ say, which specifies the plateau headway as a function of the upstream headway, for both accelerating and decelerating traffic. The qualitative difference between the maps of the stable ($a\geqslant 2.0$) and unstable ($a<2.0$) regimes is significant as shown in Fig. 10. The line $4-b_+$ that represents the invariance of Eq. (12) under the transformation (13) cuts the curve of the Bando waves only for $a<2.0$. The intersections tell us how to fit Bando waves for accelerating and decelerating traffic together to obtain the traveling jam fronts of stop-and-go traffic. Starting with an arbitrary headway b_- of, say, decelerating traffic for $a=1.0$, the map gives the corresponding headway b_+ of the plateau and hence the Bando wave. Now using this as the new headway b_- for accelerating traffic, we obtain the corresponding headway for the next Bando wave.

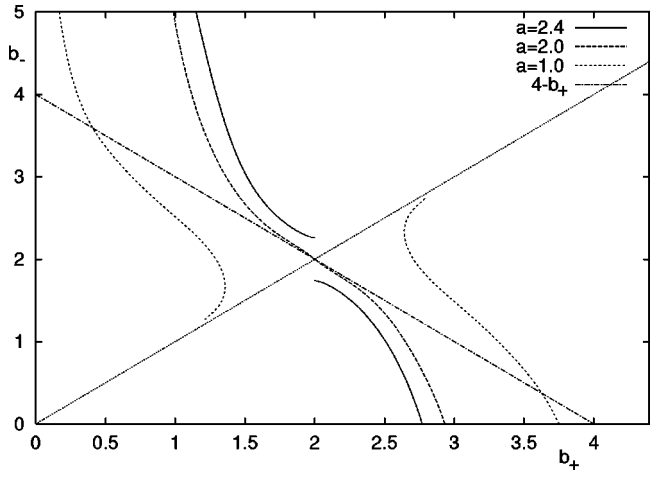

FIG. 10. Phase diagram of the Bando wave for different sensitivities a. Only for $a<2$ can they be fitted together to yield the typical jam fronts of unstable flow.

Therefore the curve defines a recursive map $b_+ = f(b_-)$ and $b_- = \overline{f}(b_+)$, respectively, for both decelerating and accelerating traffic. Iteration leads to two fixed points, which correspond to the intersections with $4 - b_+$, and this gives the stop-and-go pattern for $a < 2.0$. For $a \geqslant 2.0$ there are no fixed points and hence no jam front pattern. This may be understood since the flow is stable and no flow breakdown appears.

Moreover, the asymptotic behavior of the curve $a = 2.0$ suggests that the fixed points are a linear function for $a \lesssim 2.0$. In fact, for an OV function Eq. (2) Komatsu's [8] results reveal that the jump Δb of headway across the wave front near $a = 2$ can be approximated by [7]

$$\Delta b = 1.581\sqrt{1 - 0.5a}. \tag{15}$$

This analysis shows that Bando waves define one class of solutions for the stable and the unstable regime. Plateau effects can also be found for various upstream headways in the unstable regime. However, when the instability sets in, eventually only two specific solutions of this class are picked out and evolve. These are the stable, nonlinear stop-and-go waves. This establishes a link between Bando waves and the work of Bando *et al.* [1,2].

IV. COMPARISON WITH OTHER OV FUNCTIONS

It is of interest to examine whether similar types of transitions occur for other OV functions. This might support the idea that the wave types found in Sec. II are an intrinsic feature of car-following models with relaxation terms based on a OV function. Kerner and Konhäuser considered a model based on traffic data that does not depend on the car number and, therefore, averages over all cars to obtain a dynamic equation of the form [4]

$$\dot{v}_n = \frac{1}{T}(V_{kk}(b_n) - v_n) \tag{16}$$

with an OV function

$$V_{kk}(b) = v_0\left[\left(1 + \exp\frac{1/b - \rho_i}{\rho_{\max}\sigma}\right)^{-1} - d\right] \tag{17}$$

and

$$d = \left(1 + \exp\frac{1 - \rho_i/\rho_{\max}}{\sigma}\right)^{-1}. \tag{18}$$

Here the parameters are estimated to have the following values based on data from the German autobahn:

$$T = 0.985 \text{ s}, \tag{19}$$

$$\rho_{\max} = 180 \text{ veh./km}, \tag{20}$$

$$v_0 = 100.8 \text{ km/h}, \tag{21}$$

$$\rho_i = 36.5 \text{ veh./km}, \tag{22}$$

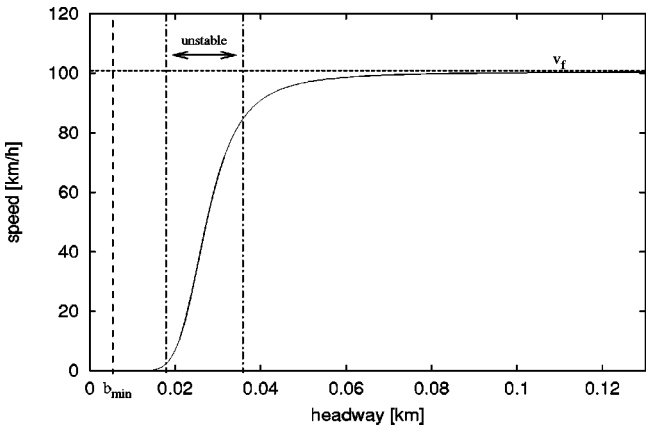

FIG. 11. The optimal velocity function $V_{kk}(b)$ of the Kerner–Konhäuser model. The flow is unstable for headways 18 m$< b <$36 m. $b_{\min}$ is the average space that cars occupy in a standstill.

$$\sigma = 0.028\,75. \tag{23}$$

$\rho_{\max}$ is the average density of cars in a jam and therefore its inverse the average length $b_{\min} = 1/\rho_{\max}$ that a car occupies. v_0 determines via $v_f := V_{kk}(\infty)$ the free flow speed. These two quantities can be measured easily. It is far more challenging to fit T, ρ_i, and σ to traffic data; one significant difficulty, amongst others, is that the flow consists of a range of different vehicles. Nevertheless this model simulates data that was obtained from a German autobahn surprisingly well [4].

In comparison to the Bando model, there are three major features which are important: the speed is only positive for headways bigger than $b_{\min}$ (Fig. 11) and by analogy the flow is only positive for densities smaller than $\rho_{\max}$ (Fig. 12). Second, the flow is unstable in a regime $b_{c_1} \approx 18$ m$< b <$36 m$\approx b_{c_2}$. These two features are different from the stable Bando model. On the other hand, one feature that the models have in common is that the flow has a turning point and this seems to be important for traveling waves as discussed in more detail above.

Figure 13 shows how linearly unstable platoons of cars with headways of 35 m and 30 m, respectively, merge. After

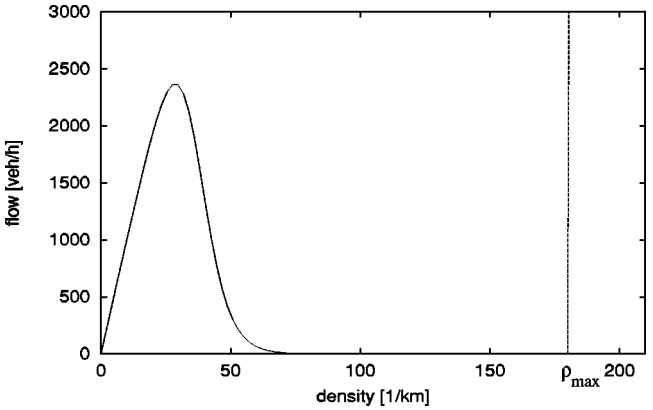

FIG. 12. Fundamental diagram: the flow vanishes for standstills ($\rho_{\max}$). The curve contains a turning point like the Bando model.

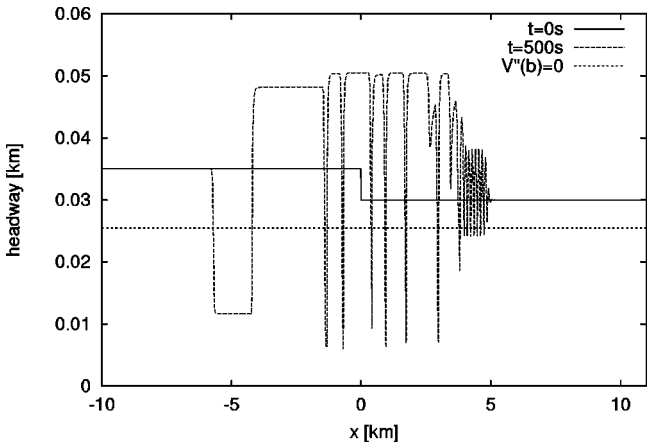

FIG. 13. The evolution of an initial jump in headway in the unstable regime. The typical jam cluster forms at the tail.

500 seconds the flow consists of clusters of vehicles with rapidly oscillating headways which are followed by the stable jam pattern of stop-and-go traffic between -6 km and -2 km. The headways of the latter, 48 m and 12 m, respectively, are not symmetric around the turning point $b_{\mathrm{tp}} \approx 26$ m $[q''(1/b_{\mathrm{tp}})=0]$ any more, since the corresponding dynamic equation (12) for the headways is not invariant under an appropriate transformation analogous to Eq. (13).

However, this system contains Bando waves for suitable upstream and downstream headways shown in Fig. 14. This nonlinear wave is formed very rapidly from the initial conditions. The Bando wave already appears before the flow becomes unstable and breaks down. Bando waves can also be found for smaller, stable upstream headways as long as the downstream headway remains stable.

In a more detailed numerical study we found most types of transitions of the stable regime as classified in Sec. II apart from the oscillatory (region II) and dispersive (region V) solutions. The oscillatory wave type could not be reproduced, even though it is observed in stable traffic flow. An explanation for this discrepancy between the model predictions and the data may be that it is necessary to introduce delay time explicitly into the dynamic equations, no matter if they are continuum or car-following models, as the Bando model Eq. (1).

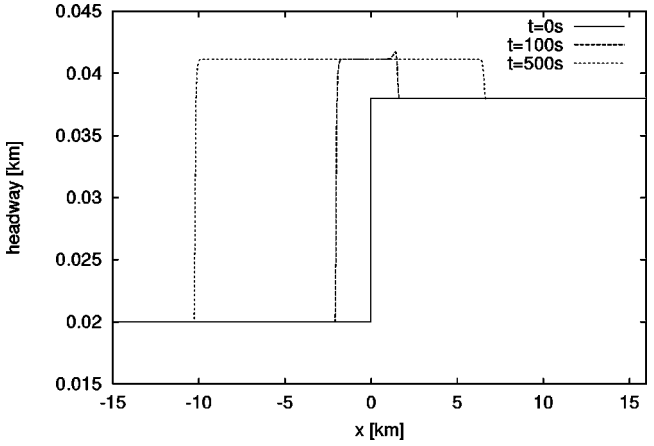

FIG. 14. Cars can adjust from an upstream to a downstream headway via a Bando wave even though parts of the headways involved in this transition are unstable.

V. PERIODIC BOUNDARY CONDITIONS

The results presented so far refer to a step function as an initial condition (Fig. 1). It is of interest to know how the profile evolves in case of periodic boundary conditions. This can either be considered as a train of density pulses along an infinitely long road or as one density pulse on a circular road.

The latter case was investigated by Nagatani [9]. He studied the relaxation process from nonuniform flow to uniform, steady flow in freely moving traffic on a circular road. Initially there are two density regions connected by kink–antikink waves. As time evolves the density profile assumes a triangular shock wave solution whose amplitude decays with time. This solution can be described by Burger's equation derived from the original optimal-velocity model [Eq. (1)] in the stable regime.

However, a triangular shock wave solution also arises from an initally uniform flow on a straight road that is disturbed by a pulselike density variation [6]. This shows that unless we are in the metastable regime [4], stable wave structures can only be found on straight roads for different values of the upstream and downstream headways $(b_{-} \neq b_{+})$. For periodic initial conditions or periodic boundary conditions (circular roads) the wave profile eventually assumes a steady, uniform flow solution. This can be explained in the phase diagrams, Figs. 2 and 5. We consider two step functions connecting regions of two different headways, say b_{high} and b_{low}, as initial conditions. This means that the profile exists of wave solutions $(b_{\mathrm{high}}, b_{\mathrm{low}})$ and $(b_{\mathrm{low}}, b_{\mathrm{high}})$, respectively, corresponding to two points in the diagrams, Figs. 2 and 5. It can be seen from Figs. 2 and 5 that at least one of these two points lies in one of the dispersive regimes. It is not possible to connect a monotonic or oscillatory wave to another one and thus obtaining a stable wave structure. Therefore, dispersion is inevitable and the wave profile eventually assumes the steady, uniform flow solution.

VI. IMPACT ON BOTTLENECKS AND AUTONOMOUS CRUISE CONTROL SYSTEMS

The effects we have discovered have significant implications for speed limits and bottlenecks. They predict that for certain jumps of headway determined by either of these measures the traffic flow locks on to a nonlinear wave. The bottleneck determines the downstream (upstream) headway, whereas the type of transition that evolves also depends on the flow further upstream (downstream). The most desirable transition in a bottleneck is the monotonic type. Oscillatory waves cause rapid breaking and acceleration which leads to higher fuel consumption and dangerous traffic situations. The same applies to Bando waves which, in addition, contain a congested region. Therefore, it might be of greater use to set up bottlenecks and speed limits stepwise along the road depending on the upstream traffic situation. Each stretch decreases the speed by a moderate and monotonic transition.

This can be a safer and more stable method than a localized large decrease in speed at a speed limit.

This has to be taken into account when implementing ACCS. The main goal of this application is to couple cars in a convoy by electronic control of their speed and acceleration by an algorithm based on a car-following law. This should result in a stable autocade of high safety and flux.

The major problems of convoy driving are the merging of cars at on- and off-ramps or at lane merging and the adjustment to bottlenecks and speed limits. All these road features have an impact on the autocade by changing the density of cars locally. From our analysis we expect transitions between these regions of different headways traveling upstream or downstream along the road. The aim of any control algorithm would be to avoid oscillatory and Bando waves.

A more realistic discussion should include the simulation of varying vehicle characteristics amongst the platoon. This represents either different driver types, cars or control algorithms. Different characteristics can be simulated by the variation of the sensitivity or the OV function as a function of the car number. This is a comprehensive, stochastic task. However, even a simple oscillatory variation of the sensitivity along the platoon reveals interesting results.

As shown in the Appendix, it only requires a few cars to cause phase transitions in the system which lead to time delays and harsh breaking maneuvers. The wave type that evolves (monotonic, oscillatory, Bando wave, etc.) depends on the composition of the vehicles with regard to their control algorithms. In a multispecies flow these vary from car to car. It is therefore harder to predict what implications a given speed limit or bottleneck has on a multispecies flow. However, the accuracy of the predictions increases when the control algorithms converge.

Speed limits which vary with time can be regarded as a changing bottleneck. They can be adjusted to the current upstream traffic situation. However, there are bottlenecks which have static characteristics such as maximum speed and throughput given by the road layout, for example. In this case optimal safety, stability, and flux might be obtained by dynamic algorithms which adjust to the downstream bottleneck situation. In-vehicle information of the oncoming traffic situation as realized by mobile technology or beacons along the road could deliver the required data.

VII. CONCLUSION

We investigated different types of wave solutions in a stable, optimal velocity model of road traffic, the Bando car-following model. Once the parameters of the model, the sensitivity and the OV function, are given, the wave types can be represented in a diagram by their upstream and downstream headways. There are six possible transitions (Fig. 2): monotonic, oscillatory, purely dispersive, shock wave plus dispersive tail, shock wave plus plateau and adjoining dispersive tail, a nonlinear shock wave plus plateau and a second shock wave.

In the latter case the two shock waves have different speeds and are separated by a growing region of congested or free flowing traffic. For sufficiently high sensitivities equivalent to small inertia, the cars react fast enough to the traffic situation and the wave does not assume this specific solution any more. For these sensitivities Bando waves and plateaus are not solutions.

For a given upstream headway the fastest traveling wave predicted from the fundamental diagram is either not accessible or, only for two specific upstream headways, just as Bando waves. In the first case its corresponding headways are either part of the dispersive regime or it locks on to a slower Bando wave.

There is a strong connection between Bando waves and traveling jam fronts of stop-and-go traffic of unstable flow. They are analogous, but while Bando waves can be found for various upstream headways for a given sensitivity, these jam fronts are uniquely determined. Jam and free flow densities are functions of the sensitivity only.

The wave types can be interpreted by the fundamental diagram. The higher the sensitivity the faster the cars react and the closer the actual dynamic flow is to the equilibrium flow. However, for small sensitivities the actual flow may differ significantly from the fundamental diagram. Therefore, an interpretation of the observed transitions is not as straightforward any more.

We compared our results to a different car-following model based on parameters fitted to real traffic data. We found all types of waves apart from the oscillatory transitions and one dispersive type due to the choice of the sensitivity parameter. It shows that the wave types we found might be an intrinsic feature of car-following models with relaxation terms.

The Bando waves play an important role when considering varying sensitivities. Once the system assumes this solution, the growing region of congested traffic between the two shock waves does not necessarily dissolve when returning to higher sensitivities. Hence, even in a linearly stable system we can find irreversible phase transitions.

This has to be taken into account when implementing autonomous cruise control systems. The algorithms must be fitted in order to avoid increasing travel times and harsh breaking maneuvers. This might be realized by dynamic algorithms which take the current downstream traffic situation into account.

ACKNOWLEDGMENTS

Peter Berg would like to thank the Alfried Krupp von Bohlen und Halbach-Stiftung and the EPSRC for their sponsorships of this project.

APPENDIX: MULTISPECIES FLOW

The advantage of discrete car-following models compared to continuum models shows when different vehicles on the road are simulated. Clearly, one has to expect new effects, as the impact of a lorry on an autocade of identical cars suggests [10].

Using the Bando model there are two ways to simulate varying vehicle characteristics: introducing functions a_n for the sensitivity or for the OV function V_n depending on the

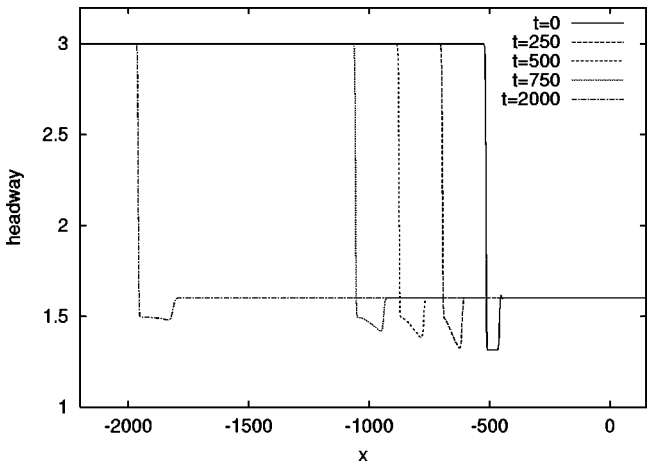

FIG. 15. Initial ($t=0$) Bando wave for $a=2.0$ followed by a convoy of cars with higher sensitivity $a=2.4$. The Bando wave changes shape but neither dissolves nor assumes the oscillatory shape as in Fig. 16.

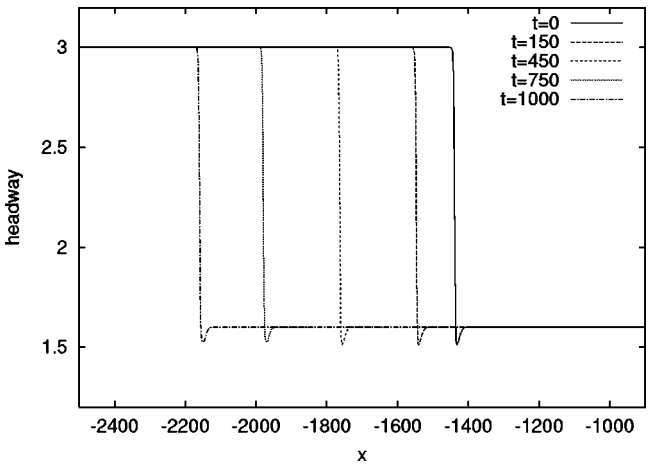

FIG. 16. Evolution of a transition from $b_-=3.0$ to $b_+=1.6$ with varying sensitivity $a_n=2.4+0.2\sin(2\pi n/100)$: the shape remains oscillatory.

vehicle number. Here, we restrict ourselves to vary the sensitivity a only. This is because we can interpret numerical results by using the diagrams Figs. 2, 4, 5, and 6.

In contrast a continuum model now contains an additional differential equation for the sensitivity and is more difficult to simulate numerically. a must be a function of space and time $a(x,t)$, since it has to travel with the cars and hence the flow. As an example we consider the analogous continuum model of the discrete Bando model as derived in Ref. [6]. In addition to the coupled, first order, partial differential equations (PDE) for density ρ and speed v,

$$\rho_t+(\rho v)_x=0, \tag{A1}$$

$$v_t+vv_x=a[V(\rho)-v]+aV'(\rho)\left[\frac{\rho_x}{2\rho}+\frac{\rho_{xx}}{6\rho^2}-\frac{\rho_x^2}{2\rho^3}\right], \tag{A2}$$

we also obtain a PDE for a. Because it must be constant for each car, we obtain simply

$$\frac{d}{dt}a(x,t)=a_t+va_x=0. \tag{A3}$$

The flow is then determined by the initial conditions

$$\rho(x,0)=\rho_0(x), \quad v(x,0)=v_0(x), \quad a(x,0)=a_0(x). \tag{A4}$$

For slowly varying sensitivities across the autocade and in the limit of small changes in headway this model is an accurate first order approach of the discrete version [6]. For randomly distributed sensitivities and rapidly changing headways as in real traffic flow, however, the solutions increasingly diverge from this model.

A classic example is a single truck of sensitivity a_{tr} surrounded by cars of a_c. Even though if the convoy is of almost uniform density and speed, the gradient of the sensitivity $(d/dx)a(x,t)$ in the continuum picture can be very large near the truck, if the distance to its neighboring vehicles is small. Already for this simple case the continuum model will fail to reproduce an appropriate picture of the actual traffic events.

In this work we varied the sensitivity as a function of the car-number n in a sinusoidal form

$$a_n=a_0+\epsilon\sin(2\pi n/N) \tag{A5}$$

and investigated how traveling waves change in shape with time. Even though it seems to be both an unrealistic distribution and very specific, it reveals that the system can go through an unexpected phase transition: once the system has switched to a certain state like the Bando wave, for example, it does not necessarily assume its initial wave solution again, an oscillatory transition for instance, that corresponds to the average sensitivity a_0. Whether a phase transition occurs or not depends in a complex manner on the parameters a_0, ϵ, n, and N.

Figure 15 shows an initial Bando wave ($t=0$) for $a=2.0$. For $t>0$ the sensitivity of the upstream cars is constantly $a=2.4$. From Fig. 4 ($a=2.4$, $b_-=3.0$, b_+

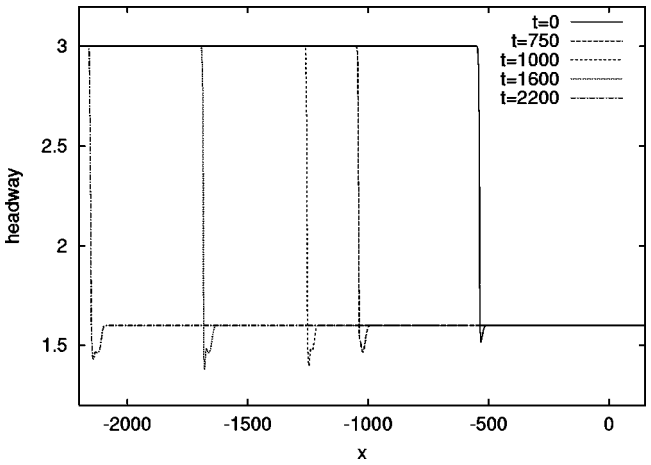

FIG. 17. Evolution of a transition from $b_-=3.0$ to $b_+=1.6$ with varying sensitivity $a_n=2.4+0.4\sin(2\pi n/100)$: Bando wave forms.

$=1.6$) we should eventually expect an oscillatory transition rather than a Bando wave. However, once the system has assumed this solution consisting of two waves, it cannot return to its initial state simply because the two waves keep going at different speeds. Thus, they do not merge into the state shown in its corresponding diagram. Only the plateau, the intermediate headway, changes its value.

Figures 16 and 17 give examples of how such a phase transition might occur. The first represents the steady state solution ($t=0$) of a transition from $b_-=3.0$ to $b_+=1.6$ and sensitivity $a=2.4$ (Fig. 4). For $t>0$ the sensitivity of the upstream cars varies like

$$a_n=2.4+0.2\sin(2\pi n/100). \tag{A6}$$

One cycle contains 100 cars and its mean is obviously $a_0=2.4$. After $t=1000$ we still find an oscillatory transition even though the cycle contains sensitivities analogous to a Bando wave. However, their percentage of the whole cycle is simply not sufficient to switch the state to this nonlinear wave.

This changes if we increase the amplitude to

$$a_n=2.4+0.4\sin(2\pi n/100) \tag{A7}$$

(Fig. 17). It still gives the same mean $a_0=2.4$ but a higher variance Δ_a

$$\Delta_a=\frac{1}{100}\sum_{n=0}^{100}(a_n-a_0)^2, \tag{A8}$$

and hence a higher percentage of those sensitivities which correspond to a Bando wave. Now there is enough time during a cycle to form a sufficiently wide gap between this wave and its corresponding downstream shock wave that does not dissolve during the next cycle. Therefore, a growing gap of varying shape forms that leads to an increase in travel time. An analogous situation appears for accelerating traffic. This leads to a decrease in travel time.

These few examples show already that a small fraction of vehicles can cause a phase transition in traffic flow. For randomly distributed sensitivities among the vehicles the mean a_0 and the variance Δ_a seem to be the two decisive variables in the system that determines what state it most likely eventually assumes. Varying sensitivities might, therefore, explain effects of traffic flow which have not been reproduced with constant sensitivity a and OV function V yet. This stochastic approach delivers plenty of problems and questions for future work.

[1] Y. Sugiyama, in *Traffic and Granular Flow*, edited by D. E. Wolf, M. Schreckenberg, and A. Bachem (World Scientific, Singapore, 1995).
[2] M. Bando, K. Hasebe, A. Nakayama, A. Shibata, and Y. Sugiyama, Phys. Rev. E **51**, 1035 (1995).
[3] B. S. Kerner and P. Konhäuser, Phys. Rev. E **50**, 54 (1994).
[4] M. Herrmann and B. S. Kerner, Physica A **255**, 163 (1998).
[5] M. J. Lighthill and G. B. Whitham, Proc. R. Soc. London, Ser. A **229**, 317 (1955).
[6] P. Berg and A. W. Woods, Phys. Rev. E **61**, 1056 (2000).
[7] E. N. Holland, Ph.D. thesis, University of Cambridge, 1996.
[8] T. S. Komatsu and S. Sasa, Phys. Rev. E **52**, 5574 (1995).
[9] T. Nagatani, Phys. Rev. E **61**, 3564 (2000).
[10] A. D. Mason and A. W. Woods, Phys. Rev. E **55**, 2203 (1997).